JEM

Supplemental material

Wray-Dutra et al., https://doi.org/10.1084/jem.20180617

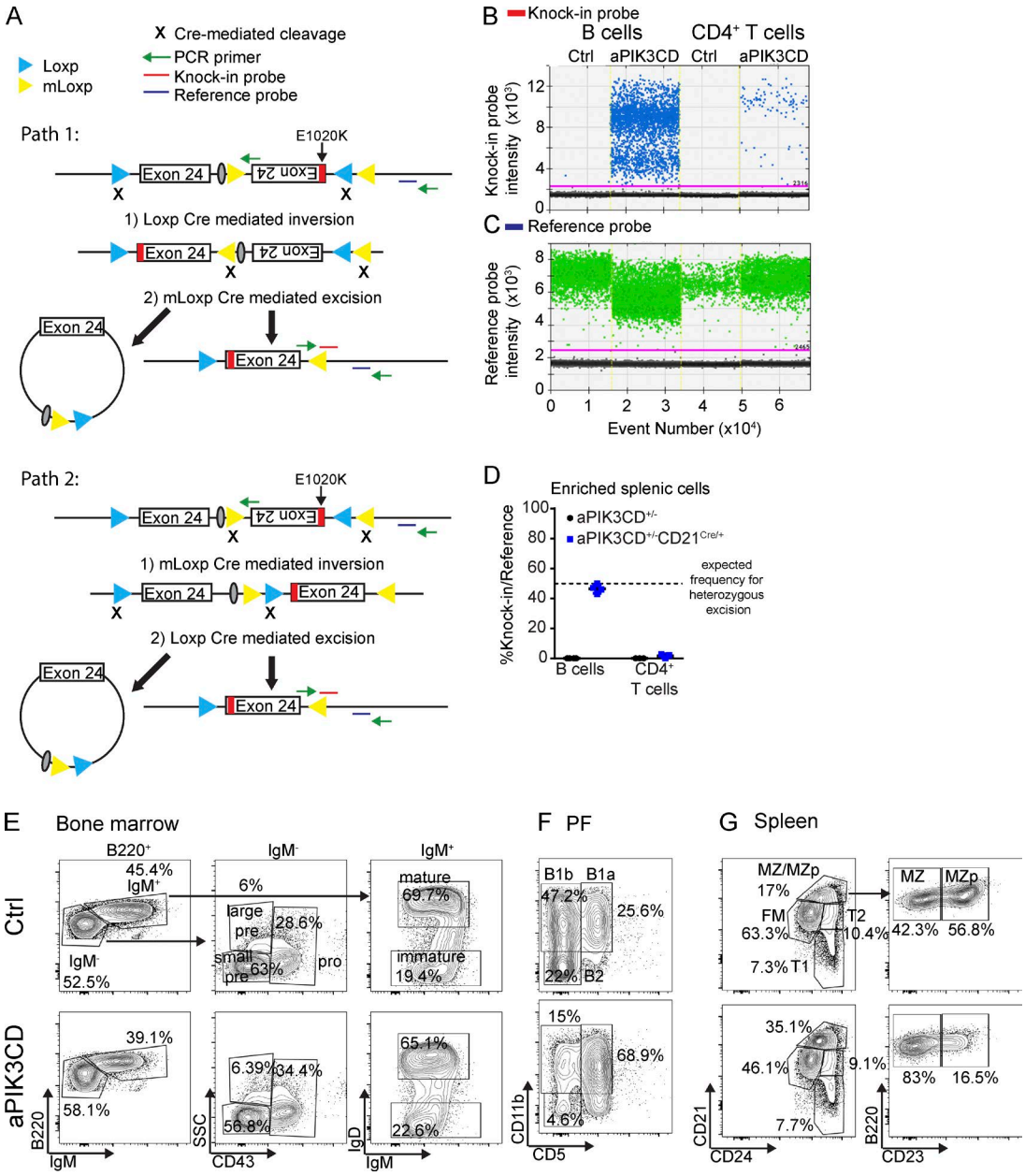

Figure S1. **Inducible PIK3CD-E1020K (aPIK3CD) murine model and representative gating strategies to identify B cell subsets in B cell–specific aPIK3CD models. (A)** Schematic of endogenous *Pik3cd* locus with Loxp-flanked endogenous exon 24 with a downstream mLoxp-flanked mutant exon 24 in the opposite orientation of transcription (3′→5′). Upon Cre-mediated excision, flipping/inversion of mutant exon 24 and excision of endogenous exon 24 can occur by two paths. Top: Path 1. Cre-mediated cleavage at Loxp sites causes flipping/inversion of mutant and endogenous exon 24, followed by Cre-mediated cleavage at mLoxp sites that results in excision of endogenous exon 24. Bottom: Path 2. Cre-mediated cleavage at mLoxp sites causes flipping/inversion of mutant exon 24, followed by Cre-mediated cleavage at Loxp sites leading to excision of endogenous exon 24. The end result of these events is fixed inversion of mutant exon 24 into the correct orientation for transcription to proceed (5′→3′). Yellow triangles: Mutant mLoxp sites; blue triangles: Loxp sites. Green arrows indicate ddPCR primer binding sites. Red line indicates knock-in ddPCR probe binding site. Blue line indicates reference ddPCR probe binding site. X indicates site of Cre-mediated cleavage. **(B–D)** B220$^+$ splenic B and CD4$^+$ T cells were purified by positive selection from 12–19-wk-old CD21$^{Cre/+}$aPIK3CD$^{+/-}$ and aPIK3CD$^{+/-}$ mice and used for ddPCR assay. **(B and C)** Representative figures showing one-dimensional amplitude ddPCR results for B cells and CD4$^+$ T cells. Blue droplets in B show binding to the knock-in junction probe. Green droplets in C show binding to the reference probe. **(D)** Frequency of knock-in probe binding normalized to reference probe binding. Expected frequency of an aPIK3CD heterozygote mouse is ∼50% (dashed line) in the presence of Cre. **(E–G)** Representative flow cytometry–based gating strategies to identify B cell subsets in Mb1-aPIK3CD and control mice. **(E)** Gating strategy for BM B cell subsets. Total B cells (B220$^+$ cells) within the viable lymphocyte gate (with doublets excluded) were gated as shown to identify pro (B220$^+$IgM$^-$CD43$^+$), large pre (B220$^+$IgM$^-$CD43$^-$SSC^{hi}), small pre (B220$^+$IgM$^-$CD43$^-$SSC^{lo}), immature (B220$^+$IgM$^+$IgD$^-$), and mature (B220$^+$IgM$^+$IgD$^+$) B cells. **(F)** Gating strategy for B cell subsets in PF. Total B cells (CD19$^+$ cells) within the viable lymphocyte gate (with doublets excluded) were next gated on total CD19$^+$cells, and CD11b^{hi} myeloid cells were excluded. B cell subsets were subsequently defined as B1a (CD19$^+$CD11b$^+$CD5$^+$), B1b (CD19$^+$CD11b$^+$CD5$^-$), and B2 (CD19$^+$CD11b$^-$CD5$^-$) B cells. **(G)** Gating strategy for splenic B cell subsets. Total B cells (B220$^+$CD24$^+$) within the viable lymphocyte gate (with doublets excluded) were gated as shown to identify early transitional (T1; B220$^+$CD24$^+$CD21^{lo}), late transitional (T2; B220$^+$CD24$^+$CD21^{int}), MZp (B220$^+$CD24$^+$CD21^{hi}CD23$^+$), MZ (B220$^+$CD24$^+$ CD21^{hi}CD23$^-$), and FM (B220$^+$CD24^{int}CD21^{int}) B cells. **(E–G)** Control (top) and (bottom) aPIK3CD.

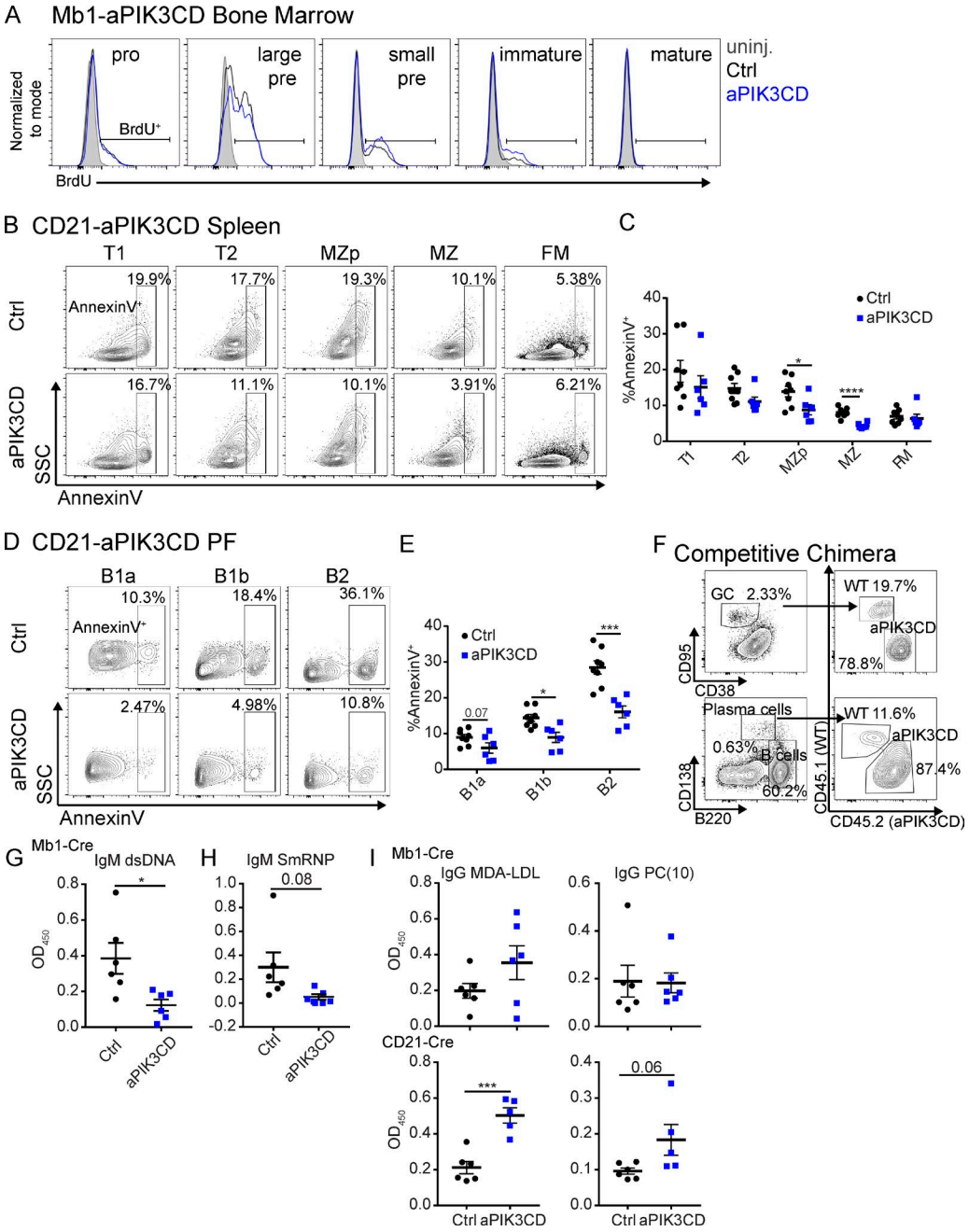

Figure S2. **Analysis of B cell cycling and survival, selection in GC and plasma cell compartments, and antibody reactivities in B cell–specific aPIK3CD models. (A)** Representative histogram overlays of BrdU⁺ cells within each BM B cell subset showing uninjected control (gray filled histogram) and BrdU-labeled control (black open histogram) and Mb1-aPIK3CD (blue open histogram) cells. Data are representative of two independent experiments. **(B)** Representative flow plots of apoptotic cells (Annexin V⁺) within splenic B cell subsets. **(C)** Quantification of frequency of apoptotic cells (Annexin V⁺) within splenic B cell subsets (MZp, P = 0.03; MZ, P < 0.0001). **(D)** Representative flow plots of apoptotic cells (Annexin V⁺) within peritoneal B cell subsets. **(E)** Quantification of frequency of apoptotic cells (Annexin V⁺) within peritoneal B cell subsets (B1b, P = 0.006; and B2, P = 0.0004). **(B–E)** Data representative of two independent experiments with eight controls and six CD21-aPIK3CD mice. **(B and D)** Control (top panels) and CD21-aPIK3CD (bottom panels) mice. Significance calculated by unpaired Student's *t* test. **(F)** Representative flow plots of WT and aPIK3CD chimerism in GC B cells (B220⁺CD95^{hi}CD38^{lo}; top panels) and plasma cells (B220⁻CD138⁺; bottom panels). Data representative of two independent experiments with seven recipient animals (CD45.1/CD45.2) at 12 wk after adoptive transfer of B cells at a 2:1 ratio of WT (CD45.1) to aPIK3CD (CD45.2) within donor BM. **(G and H)** Double-stranded DNA reactive IgM (P = 0.02; G) and Smith-ribonucleoprotein reactive IgM (H) optical density in control (black) and Mb1-aPIK3CD (blue) mice 12–13 wk of age at 1:200 serum dilution. Data representative of two independent experiments with six controls and six Mb1-a mice. Significance calculated by unpaired Student's *t* test. **(I)** Optical density of serum MDA-LDL– (left panel) and PC(10)-specific total IgG (right panel) in control versus Mb1-aPIK3CD mice (top panels). Optical density of serum MDA-LDL– (left panel; P = 0.0004) and PC(10)-specific total IgG (right panel) in control versus CD21-aPIK3CD mice (bottom panels). Significance calculated by unpaired Student's *t* test. Data representative of two independent experiments with six controls versus six Mb1-aPIK3CD mice (top panels) and six controls (Cre-negative littermates 18 wk of age) versus six CD21-aPIK3CD mice (bottom panels). *, P < 0.05; **, P < 0.01; ***, P < 0.001; ****, P < 0.0001. For summary graphs, lines indicate mean ± SEM.

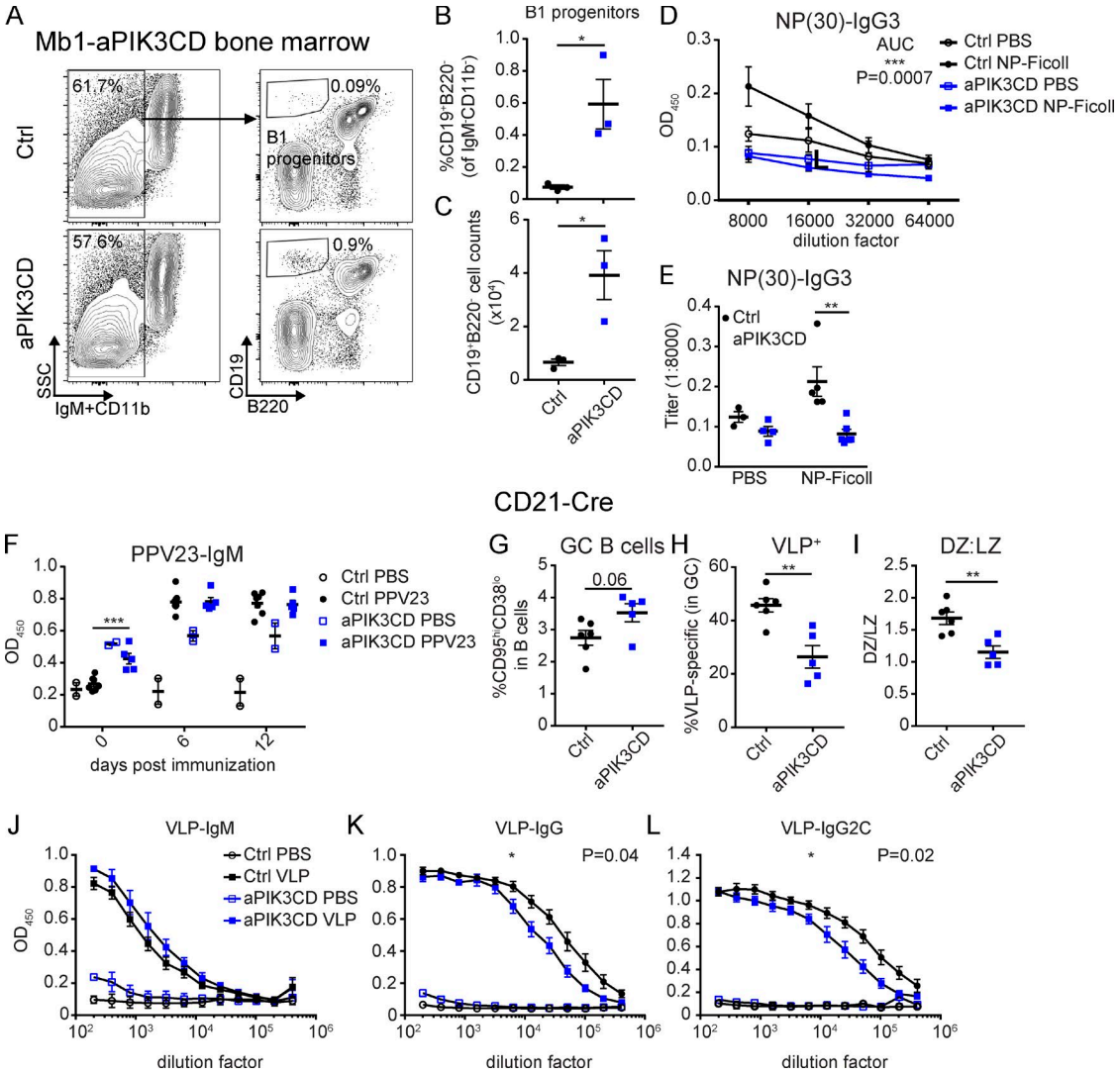

Figure S3. **B1 progenitor expansion, blunted TI-II antibody responses, and TD response in B cell–specific aPIK3CD models. (A)** Representative flow plots of B1 progenitors ($CD19^+B220^-CD11b^-IgM^-$) in BM of control (top panels) and Mb1-aPIK3CD (bottom panels) mice. **(B)** Frequency of B1 progenitors in BM (P = 0.03). **(C)** Absolute cell counts of B1 progenitors in BM (P = 0.02). **(A–C)** Data are representative of one experiment with three controls (black) and three Mb1-a (blue) mice ∼12 wk of age. Significance calculated by Student's *t* test. **(D)** Serum dilution curves of antigen-specific (NP-30) IgG3 at 7 d after injection with PBS or NP-Ficoll. Unpaired Student's *t* test of AUC (P = 0.0007; baseline = 0.0362). Open black circles: control injected with PBS; filled black circles: control injected with NP-Ficoll; open blue squares: Mb1-aPIK3CD injected with PBS; filled blue squares: Mb1-aPIK3CD injected with NP-Ficoll. **(E)** End point titers of antigen-specific (NP-30) IgG3 of 1:8,000 serum dilution at 7 d after injection (P = 0.001). Significance calculated by two-way ANOVA. **(D and E)** Data representative of two independent experiments with three PBS- and five NP-Ficoll–injected controls and four PBS- and six NP-Ficoll–injected Mb1-aPIK3CD mice. **(F)** OD_{450} of PPV23 reactive IgM in serum at days 0, 6, and 12 after immunization (day 0, PPV23, P = 0.0005). Black open circles: control PBS-injected (*n* = 2); black filled circles: control PPV23-injected (*n* = 7); blue open squares: Mb1-aPIK3CD PBS-injected (*n* = 2); blue filled squares: Mb1-aPIK3CD PPV23-injected (*n* = 5). **(G–L)** Control and CD21-aPIK3CD mice were injected i.p. with PBS or 2 µg of VLPs containing TLR7 ligand in 250 µl and sacrificed 14 d after immunization. **(G and H)** Frequency of GC B cells (G) and VLP-specific cells (H) in GC (P = 0.003). **(L)** DZ to LZ ratio within GC (P = 0.004) at 14 d after immunization. Black: control; blue: CD21-aPIK3CD. Significance calculated by Student's *t* test. **(J–L)** Dilution curves of serum VLP-specific IgM (J), IgG (K; P = 0.04), and IgG2C (L; P = 0.02). Significance calculated by Student's *t* test of AUC (baseline of 0). **(G–L)** Data representative of two independent experiments with six control mice injected with VLPs and five CD21-aPIK3CD mice injected with VLPs at 13–16 wk of age. *, P < 0.05; **, P < 0.01; ***, P < 0.001. For summary graphs, lines indicate mean ± SEM. For dilution curves, lines indicate mean ± SEM.